ISSN 0869-5911, Petrology, 2006, Vol. 14, No. 1, pp. 81–97. © Pleiades Publishing, Inc., 2006.
Original Russian Text © I.Yu. Annikova, A.G. Vladimirov, S.A.Vystavnoi, D.Z. Zhuravlev, N.N. Kruk, E.N. Lepekhina, D.I. Matukov, E.N. Moroz, S. V. Palesskii, V.A. Ponomarchuk, S.N. Rudnev, S.A. Sergeev, 2006, published in Petrologiya, 2006, Vol. 14, No. 1, pp. 90–108.

U–Pb and $^{39}Ar/^{40}Ar$ Dating and Sm–Nd and Pb–Pb Isotopic Study of the Kalguty Molybdenum–Tungsten Ore–Magmatic System, Southern Altai

I. Yu. Annikova*, A. G. Vladimirov*, S. A. Vystavnoi*, D. Z. Zhuravlev, N. N. Kruk*, E. N. Lepekhina***, D. I. Matukov***, E. N. Moroz*, S. V. Palesskii****, V. A. Ponomarchuk****, S. N. Rudnev*, and S. A. Sergeev*****

**Institute of Geology, Siberian Division, Russian Academy of Sciences, pr. Akademika Koptyuga 3, Novosibirsk, 630090 Russia*
e-mail: vladimir@iuggm.nsc.ru
***Institute of Mineralogy, Geochemistry, and Crystal Chemistry of Rare Elements, ul. Veresaeva 15, Moscow, 121357 Russia*
****Karpinskii All-Russia Research Institute of Geology (VSEGEI), Srednii pr. 74, St. Petersburg, 199106 Russia*
e-mail: sergeev@mail.wplus.net
*****Analytical Center, United Institute of Geology, Geophysics, and Mineralogy, Siberian Division, Russian Academy of Sciences, pr. Akademika Koptyuga 3, Novosibirsk, 630090 Russia*
e-mail: vitally@uiggm.nsc.ru

Received October 11, 2004

Abstract—The Kalguty ore–magmatic system comprises two intrusive complexes: the Kalguty granite–leucogranite complex and Eastern Kalguty complex of dikes and small intrusions. U–Pb dating of individual zircon grains from granites of the main intrusive phase demonstrated that the crystallization age of small grains of magmatic habits and outer rims of large grains is almost concordant and is 216 ± 3 Ma. Ar–Ar isotope study shows that the K–Ar system of biotites from granites of the main phase within the Kalguty ore field was disturbed (radiogenic Ar was partially lost) and gave an age of 202 ± 1 Ma. The Ar–Ar dating of muscovites from intraore and postore dikes of the Eastern Kalguty complex devoid of signatures of postmagmatic recrystallization and superimposed greisenization gave similar ages of 205–201 Ma. This date is considered as the emplacement age of the Eastern Kalguty dikes and associated complex W–Mo–Bi–Be ore mineralization. Sm–Nd and Pb–Pb isotopic study of granites, ongonites, and elvans of the Kalguty ore-magmatic system and host rocks shows that these systems were closed. For example, recalculation of Nd isotopic ratios for corresponding ages of crystallization of magmatic systems (216 and 205 Ma) shows that $\varepsilon_{Nd}(T)$ values decrease from –1.9 to –3.5 … –5.08 with transition from granite–leucogranite to subvolcanic granite porphyry, ongonite, and elvan dikes with corresponding increase of model ages of protoliths from 1.0 to 1.25 Ga. Lead isotopic ratios for leaching residues of whole-rock samples of all rock varieties ($^{206}Pb/^{204}Pb$ = 18.305–18.831; $^{207}Pb/^{204}Pb$ = 15.527–15.571) are plotted well below the line of average crustal lead evolution according to the Stacey–Kramers model.

DOI: 10.1134/S0869591106010073

INTRODUCTION

Estimating periods of activity of magmatic ore-forming processes and role of mantle components is very important in study of ore-magmatic systems. The mantle components could directly contribute to the formation of large and giant deposits, or multiple ascents of mantle magmas could rise geothermal gradients in lower crust and induce remobilization of ore components. Significant progress in solution of these problems has been made in studies of copper-porphyry and molybdenum-porphyry deposits (Andes, Central Asia). It was demonstrated for these deposits that combination of U–Pb and Ar–Ar isotopic dating can help in estimating the effect of postcrystallization metasomatic processes on the state of isotopic systems used in geochronology. This effect is particularly strong in the magmatic complexes located within ore fields, and some "apparent", supposedly geologically meaningless age values can be obtained. The primary Nd, Pb, and Sr isotopic ratios that are indicative of the rock origin and their site in the mantle–crust system can also be disturbed. In this paper, we would like to consider these problems for the case of the Kalguty Mo–W ore-magmatic system, Southern Altai. The Kalguty belongs to the most complex genetic type of ore-magmatic systems combining features of typical porphyry and rare-metal deposits. There are geological data for this deposit on intraore emplacement of explosive pipes, as

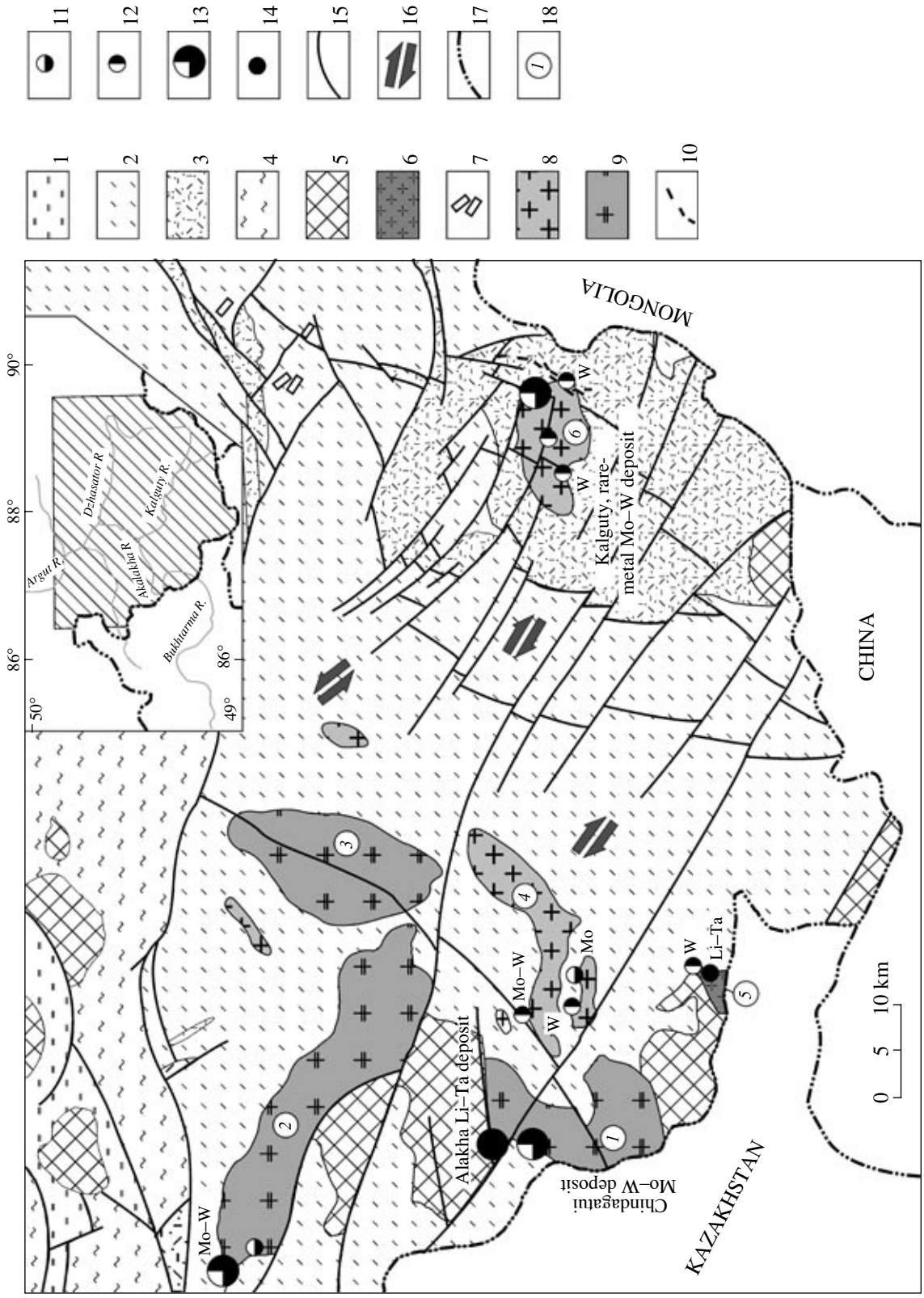
11
12
13
14
15
16
17
18
1
2
3
4
5
6
7
8
9
10
MONGOLIA
CHINA
KAZAKHSTAN
90°
88°
86°
50°
49°
86°
Argut R.
Dzhasator R.
Akdalakha R.
Kalguty R.
Bukhtarma R.
Kalguty, rare-metal Mo–W deposit
Alakha Li–Ta deposit
Chindagatui Mo–W deposit
Mo–W
Mo
Li–Ta
W
0 5 10 km

well as ongonite and elvan dikes. In this respect, the Kalguty presents the ore-magmatic system with efficient differentiation in deep-seated chambers and direct participation of mantle heat and components in ore-forming processes. Our main tasks were as follows: (1) U–Pb and Ar–Ar isotopic dating of rare-metal granites, ongonites, and elvans of the Kalguty ore-magmatic system, (2) interpretation of isotopic data and their correlation with geologic structure of the ore-magmatic system, and (3) analysis of Nd and Pb isotopic compositions as indicators of crustal and mantle magma-generating sources.

GEOLOGIC SETTING, STRUCTURAL FEATURES, AND GEOCHRONOLOGIC CHARACTERISTICS OF THE KALGUTY ORE-MAGMATIC SYSTEM

The Southern Altai is regarded now as a part of the Altai–Mongolian microcontinent with Late Proterozoic sialic basement (Berzin *et al.*, 1994; Kruk *et al.*, 1999; Buslov *et al.*, 2003). Its geologic structure within the Russian territory comprises two structural levels (Fig. 1), i.e., Early Paleozoic generally terrigenous sequences of the Gorno-Altaisk Series ($Є_3$–O, 4000–5000 m thick) and Middle Paleozoic red rock volcano-sedimentary sequences ($D_{1–2}$, 2000–2500 m thick) overlying Early Caledonian strata with stratigraphic and structural unconformity. The Middle Paleozoic rocks associate with calc-alkaline granitoids of meso- and hypabyssal facies (Shokal'skii *et al.*, 2000). The Late Paleozoic to Early Mesozoic rare-metal granites, ongonite, and elvans are sharply discordant to the older, Early to Middle Paleozoic structural–lithologic complexes. Previously, they were correlated with Kalba-type granites in Eastern Kazakhstan and, thus, dated at Permian (Amshinskii, 1973). Some K–Ar data obtained since 1970s indicated Early Mesozoic age of the Kalguty ore field (Morozov, 1986; Luzgin, 1988). In early 1990s, V.B. Dergachev and I.Yu. Annikova initiated K–Ar isotopic dating of the main rock and ore varieties of the Kalguty deposit, which verified their Late Triassic–Early Jurassic age (197 ± 20 Ma by 19 analyses). However, this conclusion had not been accepted by specialists in regional geology, magmatism, and metallogeny of the Gornyi Altai Range. Only in five years, when new geochronologic data were obtained and double-checked by U–Pb, Rb–Sr, and Ar–Ar methods for spodumene granite porphyry of the Alakha stock, it became obvious that the Early Mesozoic stage is a real benchmark in the history of the region and is most productive for rare-metal mineralization in the Southern Altai (Kozlov *et al.*, 1991; Il'in *et al.*, 1994; Vladimirov *et al.*, 1997, 1998; Kostitsyn *et al.*, 1998). Using these data, Vladimirov *et al.* (1998) and Shokal'skii *et al.* (2000) distinguished the Chindagatui–Kalguty complex of rare-metal granites and two rich rare-metal ore-bearing complexes of dikes and small intrusions: Eastern Kalguty (Mo–W ± Sn ± Cs) and Alakha (Li–Ta–Cs ± Sn ± W). All these complexes were dated at Early Jurassic, and rare-metal-rich and associated economic-grade rock varieties were considered as differentiates of parental granitic magmas. In our paper, we consider only the Kalguty ore-magmatic system. New isotopic geochronologic and geochemical data (U–Th–Pb, K–Ar, and Sm–Nd isotopic systems) allowed us to imply two-stage evolution of the ore district and verify important role of mantle components in the formation of late ongonites, elvans, and associated complex W–Mo–Be mineralization.

The Kalguty rare-metal granite massif is situated in the middle of the Kalguty tectonic depression filled with volcano-sedimentary sequences of the Early–Middle Devonian Aksai Formation (Fig. 2). The total area of the massif is 70 km^2. Two intrusive stages are distinguished in its structure. The rocks of the earlier stage (the Kalguty complex) compose >90% of the massif area. They are porphyritic biotite granites of the main phase, two-mica and muscovite leucogranite of supplementary intrusions, and aplite and pegmatite veins of the final phase. The later stage (the Eastern Kalguty complex) is represented by a dike swarm of apatite- and fluorite-bearing granite porphyry, elvans, and ongonites, including rich rare-metal varieties termed kalgutites because of specific mineralogic composition and

Fig. 1. Location of Early Mesozoic rare-metal granites, ongonites, elvans, spodumene granite porphyry, and related ore deposits in the Southern Gornyi Altai Range.

(1) Structural–lithologic complexes of the Vendian–Early Cambrian accretionary prism in the Gornyi Altai Range; (2–4) Kholzun–Chuya terrane within the Altai–Mongolian microcontinent: (2) lower structural level, Early Paleozoic turbidite sequences, (3) upper structural level, Middle Paleozoic volcano-sedimentary sequences, (4) collisional suture, Southern Chuya metamorphic complex ($PZ_{1–2}$); (5) Middle Paleozoic collisional granitoids, calc-alkaline within the Kholzun–Chuya terrane and monzonitic within the Southern Chuya collisional suture; (6–10) Early Mesozoic igneous complexes of intraplate tectonic stage: (6) granites and leucogranites of the Kungurdzharin complex (T_2kg), (7) lamprophyres and alkali basalts of the Chuya complex ($T_2č$), (8) granites and leucogranites of the Kalguty complex (T_3–J_1kl), (9) granites and leucogranites of the Chindagatui complex ($J_1čn$), (10) granite porphyry, elvans, and ongonites of the Eastern Kalguty complex (J_1vk); (11–14) rare-metal hydrothermal and magmatic ore occurrences and deposits: (11) generally Mo, (12) generally W, (13) Mo–W, (14) Li–Ta; (15) Early Mesozoic strike-slip and normal faults; (16) dominant strike-slip fault kinematics in various geoblocks (lithons); (17) frontiers; (18) massifs (numbers in map): (1) Chindagatui, (2) Orochagan, (3) Akalakha, (4) Tekekundei, (5) Kungurdzharin, (6) Kalguty. Inset shows location of the studied region.

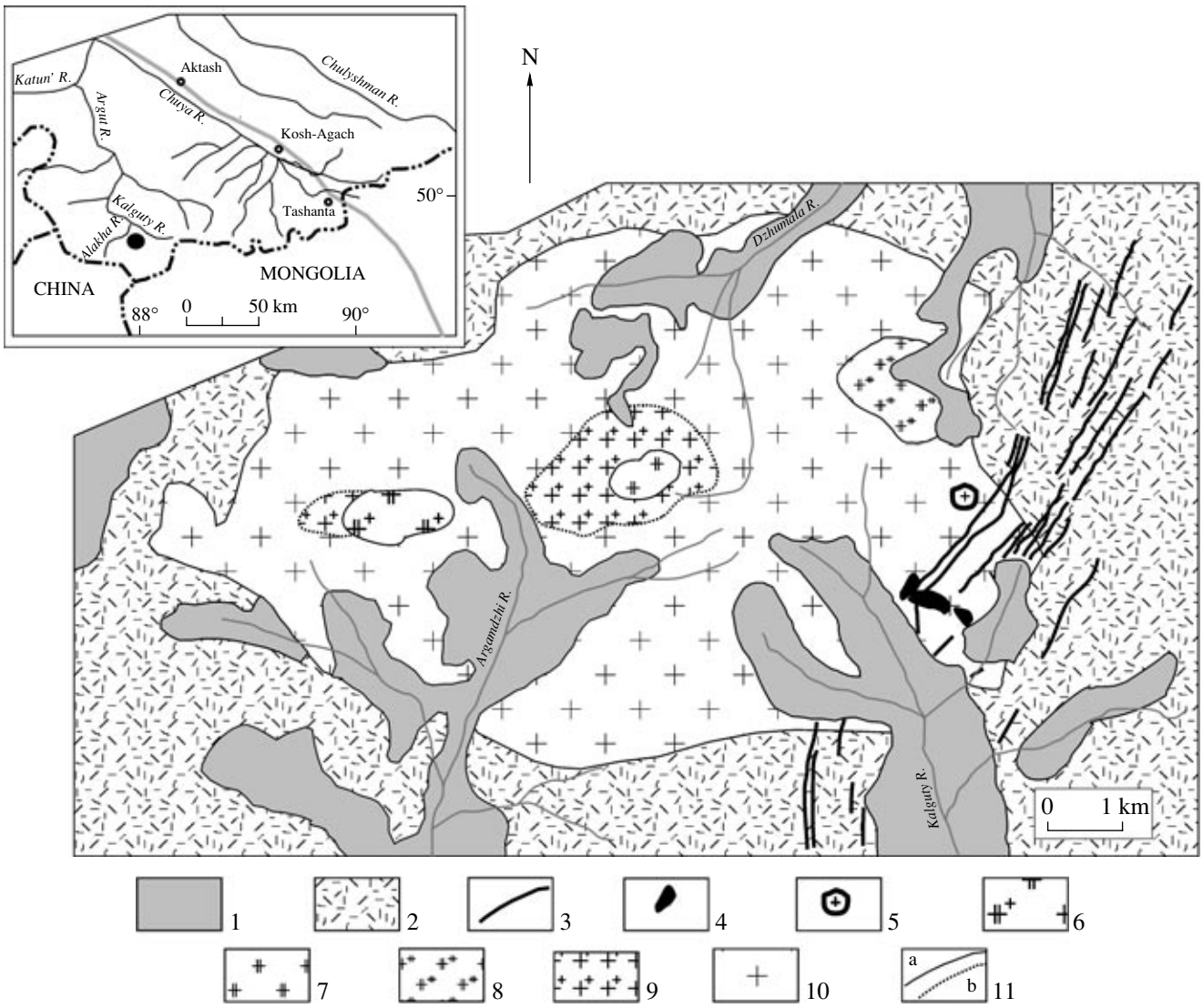

Fig. 2. Geologic scheme of the Kalguty massif of rare-metal granites, ongonites, and elvans.
(1) Quaternary deposits; (2) Devonian volcano-sedimentary rocks; (3–5) Eastern Kalguty complex: (3) elvan and ongonite dikes; (4) subvolcanic granite porphyry stocks; (5) microgranites, greisenized microgranites, and quartz–muscovite greisens of the Molybdenum stock; (6–8) Kalguty granite–leucogranite complex: phase of supplementary intrusions including (6) porphyritic two-mica leucogranites, (7) porphyritic and (or) heterogranular two-mica leucogranites, and (8) coarse-grained muscovite leucogranites; (9, 10) Kalguty granite–leucogranite complex: main intrusive phase including (9) porphyritic two-mica granites and (10) porphyritic biotite granites; (11) geologic boundaries: (a) sharp intrusive and (b) facies.
Inset shows location of the Kalguty massif.

crystallization of apatite instead of topaz (Dergachev, 1988). Granite porphyry, ongonites, and elvans of the Eastern Kalguty complex cut not only the granites and leucogranites of the earlier stage, but also quartz veins with economic-grade Mo–W mineralization related to these rocks (Annikova *et al.*, 1999). The latest generations of the elvan, ongonite, and kalgutite dikes are intraore or postore, and their alternation with W–Mo and W–Mo–Be ore veins is accompanied by general increase in concentrations of ore components both in dikes and ore veins. This is probably related to multiple release of a deep-seated chamber (or chamber system) accumulated significant amounts of ore-bearing fluids. This model is consistent with geological observations showing that the earliest granite porphyries of the Eastern Kalguty complex are cut by an explosive breccia pipe with rich Mo mineralization (Molybdenum stock) (Dashkevich *et al.*, 1991). Documentation of mine workings revealed close spatial and temporal relation of ongonites and elvans with the richest W–Mo and complex W–Mo–Be mineralization (Annikova, 2003) (Fig. 3).

Granites and leucogranites of the Kalguty complex (hypabyssal facies) show porphyritic, hypidiomorphic

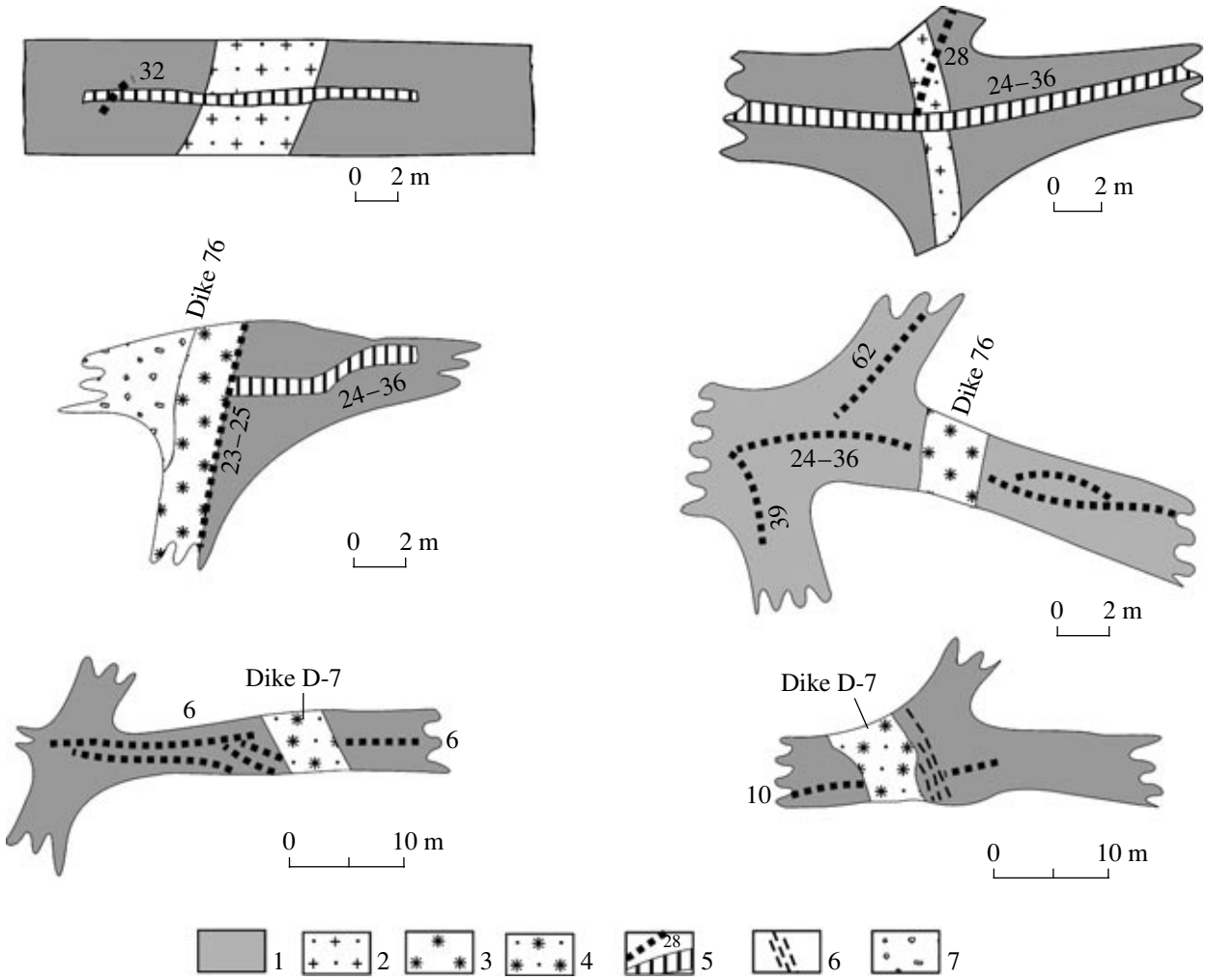

Fig. 3. Geologic relationships of granites, ongonites, elvans, and ores of the Kalguty ore-magmatic system.
(1) Porphyritic biotite granites of the main intrusive phase; (2) elvans; (3) rich rare-metal ongonites (kalgutites); (4) rich rare-metal elvans; (5) economic-grade ore-bearing quartz veins and their numbers; (6) brecciation zone, (7) talus deposits.

granular, or aplitic textures. They are generally composed of quartz, potassium feldspar, sodic plagioclase, and biotite. The rocks of the Kalguty complex are distinctly peraluminous with Shand index exceeding 1.1, have normal or some elevated alkalinity ($K_2O + Na_2O$ = 7.6–8.0 wt %), and show continuous trends in Harker diagrams (Annikova, 2003). Geochemical type of this association is not certain. Elevated P_2O_5 (0.12–0.26 wt %), Cs, Mo, W, Sr, Ba, and low F and Sn contents in granites prevent its classification with lithium–fluorine type after (Kovalenko, 1977). The rock compositions in the temporal sequence of granite–leucogranite–aplite evolve with decreasing K/Na (1.56–0.94), increasing Rb/Sr (2–5) and F content (0.07–0.1 wt %), decreasing total REE contents (166–35 ppm) and slope of chondrite-normalized REE patterns, and increasing negative Eu anomalies (Fig. 4). This fractionation type along the "albite trend" is typical of rare-metal granite magmas and is consistent with results of thermobarogeochemical studies, except for rich rare-metal ongonites (kalgutites) and elvans (Titov *et al.*, 2001). Biotites from granites of the main phase of the Kalguty complex are moderately ferrous (f = 0.495–0.517), low aluminous (Al mole fraction is 0.22–0.229), and have elevated TiO_2 (2.40–2.66 wt %) and F (1.39–1.57 wt %) and very low Cl contents. According to these parameters (Aque and Brimhall, 1987; Budnikov *et al.*, 1993), parental magma for the Kalguty complex corresponded to strongly contaminated I-type granites.

Elvans, ongonites, and kalgutites have porphyritic and (or) glomeroporphyritic textures typical of subvolcanic dike rocks with banded and fluidal varieties at the dike contacts. Quartz, potassium feldspar, sodic plagioclase, muscovite, and apatite phenocrysts are surrounded by fine- to micro-grained quartz–muscovite groundmass. Biotite more abundant in elvans is low ferrous (f = 0.391–0.426) and low aluminous (Al mole fraction is 0.209–0.212), has high TiO_2 (3.75–4.07 wt %) and F (1.63–1.90 wt %), and low Cl (0.04 wt %) con-

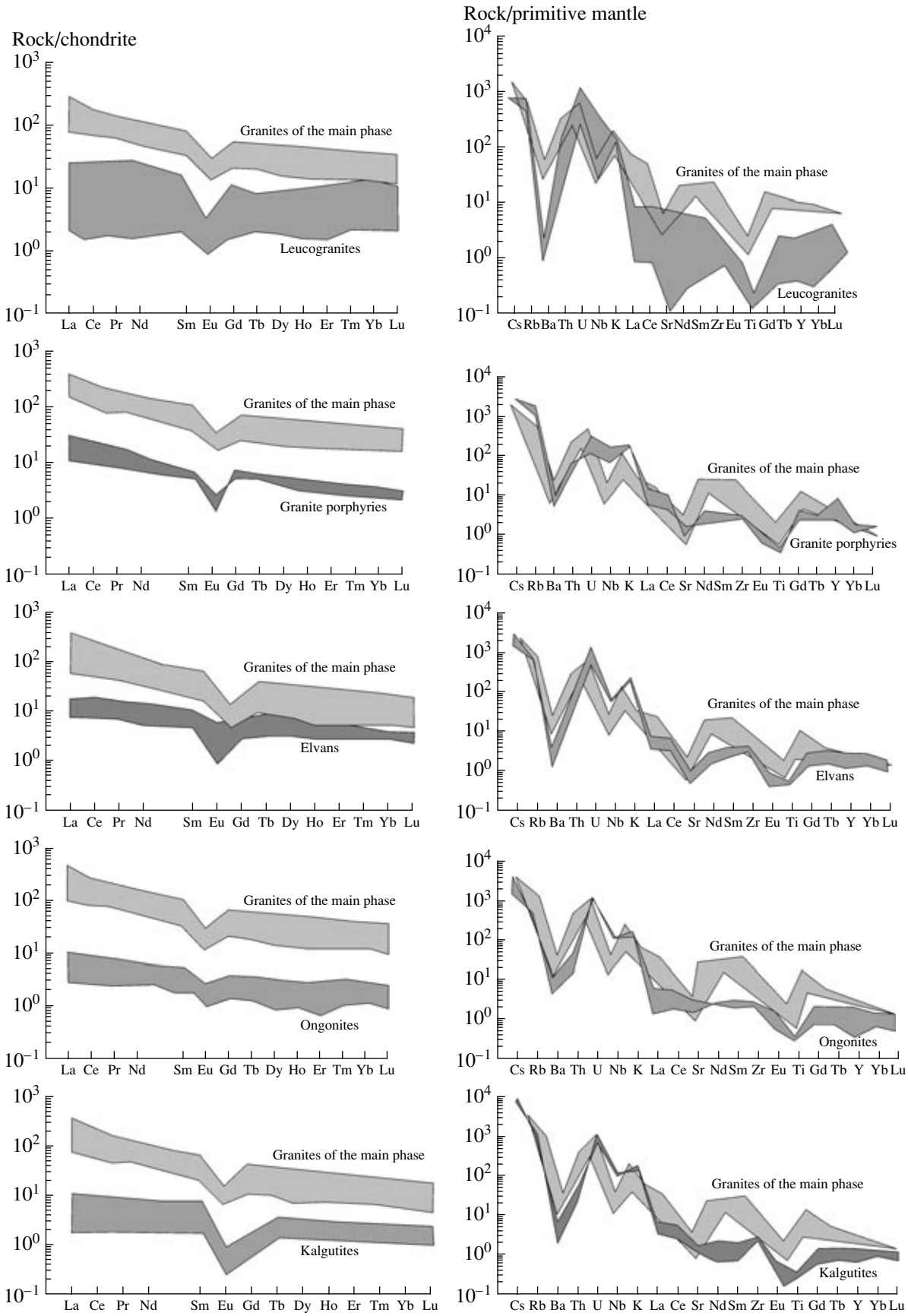

Fig. 4. Distribution of REE and spidergrams for rocks of the Kalguty ore-magmatic system.

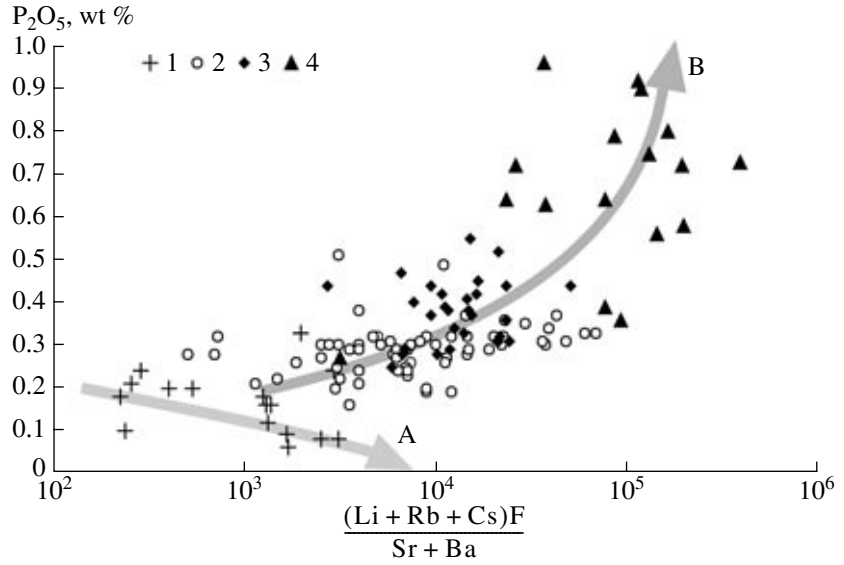

Fig. 5. $P_2O_5 - \frac{(Li + Rb + Cs)F}{Sr + Ba}$ diagram for rare-metal granites, elvans, and ongonites of the Kalguty ore-magmatic system.

(1) Porphyritic biotite granites of the main intrusive phase and leucogranites of phase of supplementary intrusions of the Kalguty complex; (2–4) Eastern Kalguty complex: (2) granite porphyry, ongonites, and elvans; (3) rich rare-metal elvans; (4) rich rare-metal ongonites (kalgutites). Arrows show trends of compositional evolution: A—Kalguty complex (low-P series) and B—Eastern Kalguty complex (high-P series).

tents. Biotites from kalgutites have elevated F contents (2.65–2.86 wt %). Muscovites of all rock varieties is free of Cl, and high F contents (up to 2.92 wt %) are found only in muscovite from kalgutites, which indicates its magmatic origin. Phosphorus contents in rocks strongly increase with transition from granites and leucogranites of the Kalguty complex to elvans, ongonites, and kalgutites of the Eastern Kalguty complex (Fig. 5). Almost all rock varieties are oversaturated in alumina (Shand index = 0.96–1.53), despite high alkali contents (up to 10 wt %). The rocks are moderately or highly ferrous, particularly, the rich rare-metal ongonites and elvans with $f = 0.80–0.85$. The latter also have high Al_2O_3 (up to 17.4 wt %), F (up to 1.16 wt %), and very high P_2O_5 (up to 0.96 wt %) contents. By these parameters, elvans and ongonites of the Kalguty ore-magmatic system are unique igneous rocks combining crustal and mantle geochemical features.

SAMPLING AND ANALYTICAL METHODS

Samples of biotite granites of the main phase of the Kalguty massif were collected for geochronologic studies from peripheral part of the Kalguty ore field: sample 1-271 (zircon and biotite fractions) and sample 1-277 (biotite fraction). The U–Pb ages of zircons were found to be significantly older than Ar–Ar ages of biotites (see below). Samples of intraore granite porphyry dikes (sample 1-278) and postore kalgutites (sample 1-262/3) were collected for age determination of the Eastern Kalguty dike complex with associated richest Mo–W and Mo–W–Be mineralization. Because of absence of notable evidence of superimposed processes, muscovite fractions comprising primary magmatic phenocrysts and groundmass laths were used for Ar–Ar isotopic dating.

Zircons were dated by U–Pb method using an ion microprobe SHRIMP-II in the Center of Isotopic Studies of the Karpinskii All-Russia Research Institute of Geology. The separated zircon grains were implanted into epoxy resin together with standard zircon grains TEMORA and 91500. Then, the zircon grains were cut by about a half of their thickness and polished. To choose analytical spots on the grain surfaces we used optical (in transmitted and reflected lights) and cathodoluminescent images showing internal structure and zoning of zircons. The cathodoluminescent images were recorded with a scanning electron microscope at working distance of 25–28 mm, accelerating voltage of 20 kV, and focused beam current of 4–6 nA on Faraday cylinder. Probe current was adjusted to get the best contrast of image at low corrosion of pellet surface due to local heating. Determination of U–Pb ratios with SHRIMP-II were performed using the procedure described in (Williams, 1998). Intensity of primary beam of negative molecular oxygen ions was 4 nA, diameter of spot (crater) was 18 μm. The data obtained were treated with SQUID code (Ludwig, 2000). The U–Pb ratios were normalized to $^{206}Pb/^{238}U = 0.0668$ in TEMORA standard zircon corresponding to the age of 416.75 Ma of this zircon (Black *et al.*, 2003). Uncertainties of individual analyses (ratios and age values)

Table 1. Results of U–Pb isotopic study of zircon from granites of the main phase of the Kalguty rare-metal granite massif (sample 1-271)

Ordinal	$^{206}Pb_c$, %	U, ppm	Th, ppm	$^{232}Th/^{238}U$	$^{206}Pb^*$, ppm	$^{206}Pb/^{238}U$[1]	$^{207}Pb/^{206}Pb$[1]
1	0.00	453	208	0.47	13.5	220.5 ± 2.1	297 ± 62
2	0.41	286	178	0.64	8.54	219.2 ± 3.4	63 ± 460
3	0.00	964	520	0.56	28.3	216.6 ± 1.5	252 ± 41
4	0.81	399	210	0.54	11.4	209.4 ± 2.3	47 ± 230
5	0.52	448	195	0.45	13.0	213.7 ± 2.1	13 ± 130
6	1.01	92	71	0.80	5.35	418.8 ± 7.8	318 ± 430
Ordinal	$^{208}Pb/^{232}Th$[1]	Measured $^{238}U/^{206}Pb$	Measured $^{207}Pb/^{206}Pb$	$^{238}U/^{206}Pb^*$[1]	$^{207}Pb^*/^{206}Pb^*$[1]	$^{207}Pb^*/^{235}U$[1]	$^{206}Pb^*/^{238}U$[1]
1	228 ± 6	28.76 ± 0.95	0.0515 ± 2.7	28.74 ± 0.95	0.0523 ± 2.7	0.2508 ± 2.9	0.03480 ± 0.95
2	199 ± 26	28.79 ± 1.10	0.0506 ± 3.4	28.91 ± 1.60	0.0473 ± 19.0	0.225 ± 20.0	0.03459 ± 1.6
3	212 ± 3	29.26 ± 0.72	0.05112 ± 1.8	29.26 ± 0.72	0.05124 ± 1.8	0.2415 ± 1.9	0.03418 ± 0.72
4	193 ± 15	30.04 ± 0.98	0.0534 ± 2.8	30.28 ± 1.10	0.0470 ± 9.8	0.214 ± 9.8	0.03302 ± 1.10
5	196 ± 10	29.51 ± 0.94	0.0505 ± 2.6	29.67 ± 0.98	0.0463 ± 5.5	0.215 ± 5.6	0.03371 ± 0.98
6	406 ± 44	14.75 ± 1.50	0.0609 ± 3.9	14.90 ± 1.90	0.0527 ± 19.0	0.488 ± 19.0	0.0671 ± 1.90

Note: Uncertainties are given at 1σ confidence level. Pb_c and Pb* are common and radiogenic lead, respectively. Error of standard calibration is 0.49%.
[1] Common lead was corrected using ^{204}Pb.

are given at 95% confidence level (σ), uncertainties of calculated concordant ages and concordia intercepts, at 99.5% confidence level (2σ). The concordia diagrams were plotted using ISOPLOT/EX code (Ludwig, 1999).

Procedure of the Ar–Ar dating is described in (Travin, 1994) and is considered here only briefly. Mineral fractions >0.15 mm were packed in aluminum foil and sealed in quartz ampoules after air removal. The samples were irradiated in Cd channel of VVR-K research reactor of the Tomsk Polytechnical Institute. Biotite sample MCA-11 calibrated using biotite LP-6 and hornblende MMhb-1 was placed between each two samples for calibration of neutron flux. Gradient of the neutron flux did not exceed 0.5% over sample area. Argon was released in a quartz reactor with an external heating furnace. A chromel–alumel thermocouple was used to control and stabilize temperature. Blank for ^{40}Ar at 1200°C during 40 min was below 5×10^{-9} ncm^3. After double purification of the separated argon using Ti and ZrAl SAES getters, Ar isotopic composition was measured using a Noble gas 5400 Micromass mass spectrometer, UK. Temperature fractions for calculation of age values using plateau method were chosen according to recommendations of Fleach *et al.* (1977). Decay constants and isotope abundances recommended by Commission on Geochronology (IUGS) (Steiger and Jager, 1976) were used in age calculations.

The Sm–Nd isotope studies were performed for whole-rock samples characterizing main types of sedimentary and metamorphic rocks of the southern part of the Gornyi Altai Range, as well as the main rock varieties of the Kalguty ore-magmatic system. Alkaline basic and lamprophyre dikes of the Chuya complex that are thought to be temporally and spatially related to rare-metal granite magmatism (Vladimirov *et al.*, 1998) were also analyzed. Sm and Nd were separated using standard techniques (Richard *et al.*, 1976). Sm isotopic composition was measured using a MI-1320 mass spectrometer, while Nd isotopes were analyzed with a multicollector Finnigan MAT-262 mass spectrometer. Neodymium isotope ratios were normalized by $^{146}Nd/^{144}Nd = 0.7219$. Uncertainty in determination of Sm/Nd ratio was ±0.2%. Replicate analyses of Nd isotopic composition of La Jolla standard gave $^{143}Nd/^{144}Nd = 0.511842 \pm 14$ by 17 determination. The specified uncertainty was used in calculations of isochrons as the most real estimate of uncertainty in analysis of Nd isotopic composition.

Lead isotopic ratios in rocks were measured in the Institute of Precambrian Geology and Geochronology, Russian Academy of Sciences, St. Petersburg. Pb and U were separated using procedure described in (Manhes *et al.*, 1984). U and Pb isotopic compositions were analyzed with a multicollector Finnigan MAT-261 mass spectrometer with simultaneous registration of currents of different isotopes. Coefficient of Pb fractionation being equal to 0.0013 ± 0.0002 amu^{-1} was obtained by multiple measurements of NBS-SRM-982 isotopic standard. Primary data were treated using PBDAT code. Isochron parameters were calculated with 95% confidence level using ISOPLOT code.

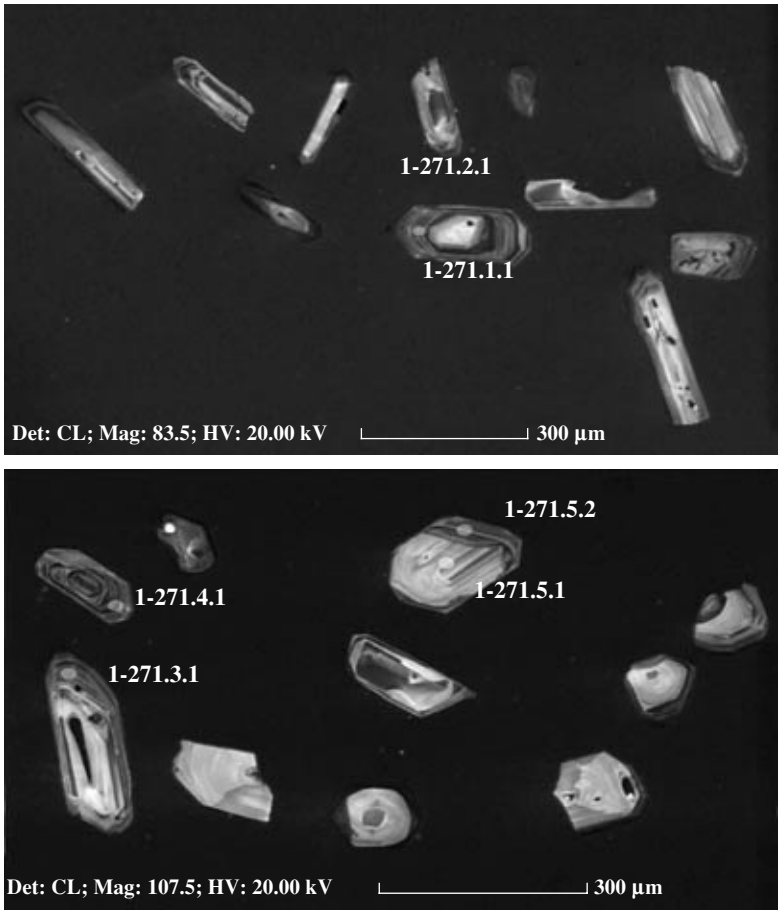

Fig. 6. Cathodoluminescent images of zircons from granites of the main intrusive phase of the Kalguty massif (sample 1-271).

RESULTS

U–Pb isotopic data for individual zircon grains from granites of the main phase of the Kalguty massif are given in Table 1. These zircons compose euhedral transparent and semitransparent occasionally fractured prismatic pale pink and light yellow crystals of hyacinth habits, K_{elong} = 1.5–3.0 (up to 4.0–5.0). Crystal faces are plane and lustrous with distinct edges. Crystals shows prismatic ({100}, {110}) and dipyramidal ({111}, {211}) faces. The grains have rough magmatic zoning, particularly in the marginal parts of crystals, and numerous gas–liquid and solid, transparent and opaque mineral inclusions. Some large crystals have rounded cores of old zircons. This conclusion was verified by study of cathodoluminescence of some zircon grains (Fig. 6). It was found that most zircon grains are magmatic and show characteristic zoning in margins, where U–Pb isotopic ratios were analyzed on SHRIMP-II (Fig. 6). These data indicate that small zircon grains (≤0.16–0.25 μm) and rims of large grains (≥0.5 μm) crystallized in magmatic stage and have ages at 216 ± 3 Ma (Table 1, Fig. 7). Some zircon grains include xenogenic domains that are distinctly discordant with respect to magmatic rims (Fig. 7). Preliminary study of these cores demonstrated that they have older age of about 400–440 Ma (at 95% confidence level) (Fig. 8). We can reliably suggest that xenogenic zircon was derived from

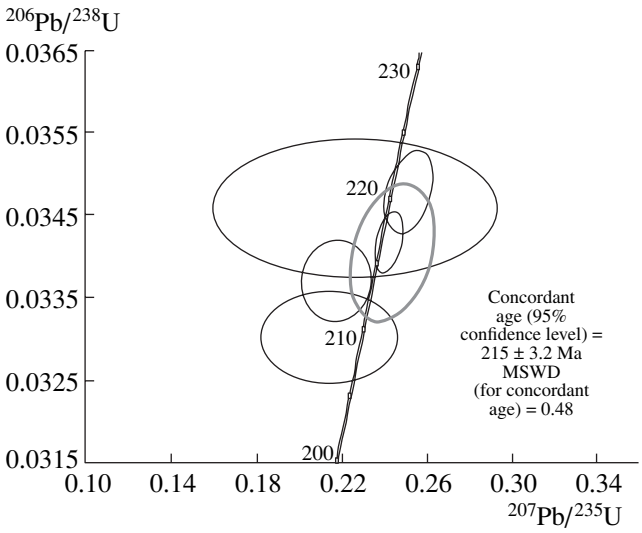

Fig. 7. U–Pb concordia diagram for zircons from sample 1-271 of granites of the main intrusive phase of the Kalguty massif. Ellipses correspond to 68.3% confidence level.

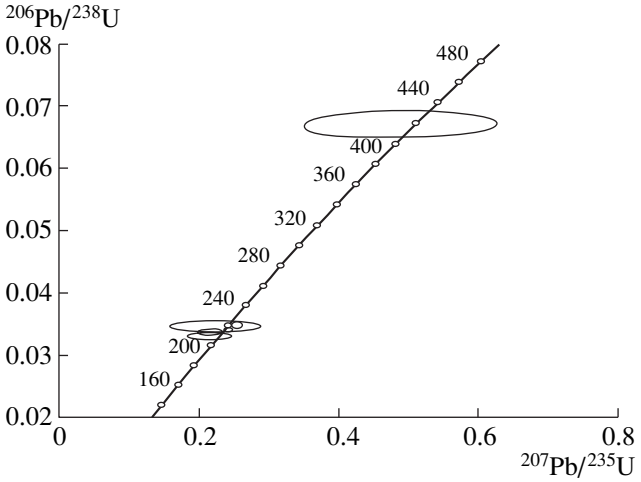

Fig. 8. U–Pb concordia diagram for xenogenic zircon from sample 1-271 of granites of the main intrusive phase of the Kalguty massif.

Note the U–Pb isotopic age of xenogenic zircon being 400–440 Ma.

xenoliths of the Early Devonian volcanic rocks of the Aksai Formation, which were captured by the Kalguty rare-metal granite magma during its ascent and crystallization. High uncertainty of age of xenogenic zircon is because of single determination, which is regarded as preliminary for future isotopic geochronologic studies.

The Ar–Ar isotopic study of biotites separated from granites of the main phase of the Kalguty complex gave ages of 202 ± 1 and 201.8 ± 0.6 Ma (Fig. 9), which differ from the U–Pb concordant age for magmatic zircon. This deviation is probably related to behavior of K–Ar system of biotite. Formal analysis of $^{39}Ar/^{40}Ar$ diagrams shows that K–Ar system of biotite was modified by loss of radiogenic Ar at later stages in evolution of the Kalguty ore-magmatic system. This could be true, because all granite samples were collected within the Kalguty ore field and muscovites from granite porphyry and ongonites of the Eastern Kalguty complex having intraore and postore geologic setting (thus being undergone much less intensive thermal and metasomatic impact than granites of the main phase) show some younger $^{39}Ar/^{40}Ar$ ages (see below).

The Ar–Ar isotopic study of muscovites separated from intraore granite porphyry and postore kalgutites of the Eastern Kalguty dike complex showed similar ages for these rocks, i.e., 202 ± 1 and 203 ± 1.5 Ma, respectively (Fig. 10). The K–Ar system in muscovite is more resistant to thermal impact than the biotite system. Thus, we can suggest that the age estimates correspond to an actual geologic process.

The Sm–Nd isotopic studies demonstrated that igneous rocks of the Kalguty ore-magmatic system typically have low primary $^{143}Nd/^{144}Nd$ ratios at always negative $\varepsilon_{Nd}(T)$ values (Table 2). The highest $\varepsilon_{Nd}(T) = -1.9$ is found for porphyritic biotite granites of the main phase of the Kalguty massif. Model age of protolith of these rocks is 1.17 Ga. The rocks of the Eastern Kalguty dike complex (elvans and kalgutites) have notably lower and variable $\varepsilon_{Nd}(T)$ (from –3.7 to –5.1). Model age of their protoliths is 1.31–1.43 Ga. The lowest $\varepsilon_{Nd}(T)$ and largest model ages of protoliths are typical of high-temperature elvans (sample 1-269).

Lead isotopic ratios were obtained for leaching residues of whole-rock samples of all rock varieties of the Kalguty ore-magmatic system. The Pb isotopic composition is low radiogenic, and isotopic ratios (except for those for galenobismuthite, sample 18) fall within narrow intervals ($^{206}Pb/^{204}Pb = 18.305–18.831$; $^{207}Pb/^{206}Pb = 15.527–15.571$) (Table 3). This means that Pb isotopic compositions of residues is close to composition of primary Pb incorporated in rocks during their formation, i.e., to isotopic composition of rock source. Using these values we calculated model lead parameters of the source, which are equal to $\mu_1 = {}^{238}U/^{204}Pb = 8.07$ and $\kappa_1 = {}^{238}U/^{232}Th = 3.27$ for one-stage evolution model and $\mu_1 = {}^{238}U/^{204}Pb = 9.47$ and $\kappa_1 = {}^{238}U/^{232}Th = 3.18$ for the Stacey and Kramers model. These data indicate significant contribution of mantle components into the rock source, because Pb isotopic ratios are plotted well below the line of average crustal lead evolution according to the Stacey–Kramers model (Fig. 11).

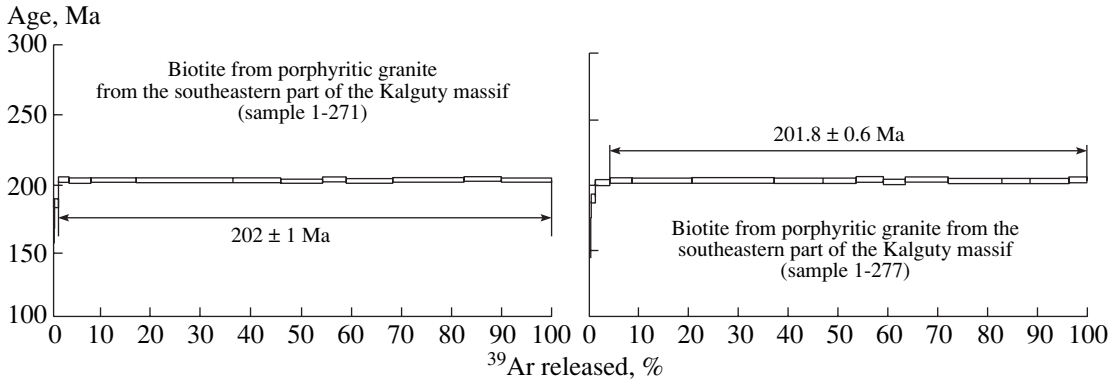

Fig. 9. $^{39}Ar–^{40}Ar$ age spectra for biotite from granite of the main intrusive phase of the Kalguty massif.

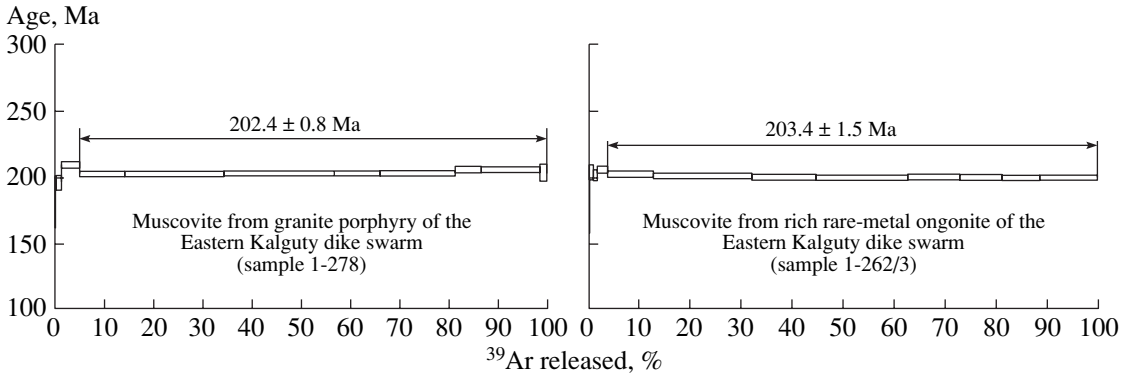

Fig. 10. ^{39}Ar–^{40}Ar age spectra for muscovite from granite porphyry and kalgutites of the Eastern Kalguty complex.

DISCUSSION

Estimation of Time Interval of Formation of the Kalguty Ore-Magmatic System and Occurrence of Deep-Seated Chambers of Rare-Metal Magma

Results of isotopic dating of individual zircon grains by U–Pb method using SHRIMP-II mass spectrometer (T = 216 ± 3 Ma), as well as biotite from granites of the main phase (T = 202 ± 1 Ma) and muscovite from granite porphyry and kalgutite dikes (205–201 Ma) by Ar–Ar method with stepped heating of mineral fractions, led us to the following conclusions.

A time gap of about 10–15 m.y. is reliably established between the emplacement of rare-metal granites of the Kalguty complex composing the main volume of

Table 2. Sm–Nd isotopic composition of rocks of the Southern Gornyi Altai Range

Ordinal	Sample	Sm, ppm	Nd, ppm	$^{147}Sm/^{144}Nd$	$^{143}Nd/^{144}Nd$	$\varepsilon_{Nd}(0)$	$\varepsilon_{Nd}(T)$	$T_{Nd}(DM)$	$T_{Nd}(DM\text{-}2st)$
1	1-277	6.57	31.9	0.1245	0.512442 ± 10	–3.8	–1.9	1212	1165
2	1-278/1	0.727	2.99	0.14709	0.512313 ± 9	–6.3	–5.0	1915	1425
3	1-259	7.06	34.6	0.12328	0.512351 ± 6	–5.6	–3.7	1348	1310
4	5-446*	1.564	5.835	0.16207	0.51235 ± 6	–5.6	–4.7	2359	1394
5	1-269	6.78	33.2	0.1234	0.51228 ± 6	–7.0	–5.1	1469	1425
6	1-262/3	2.05	9.31	0.13303	0.512373 ± 9	–5.2	–3.5	1469	1295
7	5-447*	0.1623	0.4368	0.2246	0.51245 ± 9	–3.7	–4.4	–	1366
8	5-401	8.034	41.78	0.11624	0.512325 ± 9	–6.1	–2.0	1292	1330
9	RA-3/3	5.576	26.78	0.12585	0.512376 ± 8	–5.1	–1.5	1345	1288
10	L-3	20.5	109.0	0.11337	0.512317 ± 9	–6.3	–3.6	1267	–
11	8-568/3	12.6	81.0	0.09418	0.512295 ± 9	–6.7	–3.4	1092	–
12	5-451	7.18	47.0	0.09238	0.512287 ± 8	–6.8	–3.5	1086	–
13	95-1/3	3.59	18.2	0.1194	0.512202 ± 7	–8.5	–6.5	1533	–
14	95-11/7	5.76	27.7	0.12565	0.512286 ± 9	–6.9	–5.0	1496	–
15	95-7/2	4.29	21.4	0.12145	0.512133 ± 7	–9.9	–7.9	1680	–

Note: (1–7) Kalguty ore-magmatic system: (1) porphyritic biotite granite of the main phase; (2–5) elvans; (6, 7) kalgutites; (8, 9) granitoids of the Rakhmanovo complex (D_{1-2}) including (8) biotite granite and (9) biotite granodiorite; (10–12) rocks of the Chuya alkali basite complex (P_2–T_1): (10) minette, (11) kersantite, (12) melanosyenite; (13–15) upper crustal metamorphic rocks of the Altai–Mongolian terrane: (13) green schist, (14) disthene–staurolite gneiss, (15) cordierite–biotite gneiss.

* Samples for which the uncertainties in $^{147}Sm/^{144}Nd$ determination can be high.

$\varepsilon_{Nd}(T)$ values are calculated relative to CHUR with present-day $^{143}Nd/^{144}Nd = 0.512638$ and $^{147}Sm/^{144}Nd = 0.1967$ (Jacobsen and Wasserburg, 1984). Model ages are calculated by model (Goldstein and Jacobsen, 1988) for depleted mantle reservoir with present-day $^{143}Nd/^{144}Nd = 0.513151$ and $^{147}Sm/^{144}Nd = 0.21365$. Calculation of protolith ages by two-stage model (Liew and Hofmann, 1988) used average crustal $^{147}Sm/^{144}Nd$ ratio of 0.12 (Taylor and McLennan, 1985). $\varepsilon_{Nd}(T)$ and $T_{Nd}(DM\text{-}2st)$ are calculated for granites at 216 Ma of the main phase of the Kalguty massif, 202 Ma for elvans and ongonites of the Eastern Kalguty dike swarm, 400 Ma for rocks of the Rakhmanovo complex, and 250 Ma for rocks of the Chuya complex. Dash denotes no data.

Table 3. Lead isotopic composition of rocks and ores of the Kalguty ore-magmatic system

Ordinal	Sample	Fraction	$^{206}Pb/^{204}Pb$	$^{207}Pb/^{204}Pb$	$^{208}Pb/^{204}Pb$	μ_{meas}	Pb, ppm	U, ppm
1	1-277	WR	18.803	15.612	38.677	15.18	29.4	6.97
2		L	20.579	15.66	39.755	71	6.34	6.82
3		R	18.309	15.527	38.192	5.53	24.7	2.17
4	1-259	WR	19.943	15.652	40.216	58.1	9.68	8.47
5		L	20.946	15.677	45.134	126.2	2.41	4.25
6		R	10.511	15.582	38.676	29.2	8.90	4.03
7	1-262/3	WR	19.911	15.618	38.433	116.5	17.2	30.9
8		L	28.491	16.087	40.498	103.2	2.14	20
9		L	28.473	16.111	40.516	–	2.13	–
10		R	18.831	15.562	38.116	3.25	30.3	1.55
11	1-278/1	WR	21.54	15.745	38.416	17.51	14.97	3.95
12		L	34.616	16.447	39.038	66.5	3.17	2.68
13		R	18.633	15.547	38.104	4.42	11.27	0.786
14	1-269	WR	18.457	15.571	38.48	17.91	32.4	9.14
15		L	19.337	15.6	39.74	122.4	4.52	8.12
16		L	19.305	15.63	39.858	–	4.35	–
17		R	18.305	15.555	38.27	2.67	29.9	1.26
18	18	galenobismuthite	18.142 ± 24	15.515 ± 19	38.166 ± 51	–	–	–

Note: WR—whole-rock sample, L—leachate in mixture of concentrated HNO_3 and HCl, R—leaching residue; 1-277 is porphyritic biotite granite of the main phase, 1-259 is elvan, 1-262/3 is rich rare-metal ongonite (kalgutite), 1-278/1 is muscovite granite porphyry, 1-269 is elvan, 18 is galenobismuthite from a quartz–molybdenite–wolframite–chalcopyrite vein. Dash denotes no data.

the Kalguty massif and the formation of subvolcanic dikes and small intrusions of granite porphyry, ongonites, and elvans. This conclusion in generally consistent with geological data, but, with allowance for geochemical similarity of all intrusive rocks and their close spatial association, it requires some comments related to interpretation of geochronologic data and development of consistent petrogenetic model of formation of the Kalguty ore-magmatic system. Let us emphasize that Ar–Ar dates coincide for biotites from granites of the main phase and muscovites from definitely later dikes. Note that samples for biotite separation were collected within ore field with widely developed greisenization. We found that the muscovite in granites of the main phase is a secondary mineral (Annikova, 2003), and we can suggest that biotite has also undergone recrystallization with disturbance of K–Ar system. On the contrary, muscovite in granite porphyry and ongonites is primary magmatic mineral and composes euhedral phenocrysts and groundmass laths (Fig. 12). Ar–Ar isotopic study of muscovites gave the age similar to the age obtained for biotite from significantly older granites of the main phase. This is consistent with intraore setting of dikes associating with the most productive complex W–Mo–Bi–Be mineralization. If we suggest that all dikes of the Eastern Kalguty complex are postore, biotite recrystallization over such large area cannot be explained. Thus, the obtained isotopic geochronologic and geologic data are consistent and may indicate that the Kalguty ore-magmatic system was formed during two stages. At the first stage (216 ± 3 Ma) corresponded to emplacement of hypabyssal fracture intrusion (Annikova *et al.*, 2004), and parental magma was differentiated due to crystal fractionation to produce granites of the main phase ⟶ leucogranites of supplementary intrusions ⟶ aplites of the final phase. This stage was accompanied by Mo and Mo–W ore mineralization. Data on Re–Os dating of molybdenite from ores within the Kalguty field gave age value of 213 Ma (Borisenko *et al.*, 2003), which, according to geologic data (Vladimirov, 1997, 1998; Shokal'skii *et al.*, 2000), coincides with the age of the earlier magmatic stage of the Kalguty ore-magmatic system of 216 Ma obtained for individual zircon grains.

Considering muscovite in granite porphyry and ongonites to be a primary magmatic mineral with K–Ar isotopic system more resistant to thermal impact than that of biotite, we can suggest that values of 202.4 ± 0.8 and 203.4 ± 1.5 Ma correspond to an actual geologic process, i.e., the formation of the Eastern Kalguty dike swarm and spatially associated complex W–Mo–Bi–Be mineralization. The time gap of 10–15 m.y. with strong changes in ore geochemistry from Mo–W to W–Mo–Bi–Be can be explained by former existence of a large slowly cooling lower crustal magma chamber, which

released magma and fluids at least twice and produced a multilevel ore mineralization in the upper crust.

Mantle Role

There are many petrologic and isotopic geochemical data accumulated recently on significant contribution of mantle plume sources in composition of rare-metal silicic magmas (Vladimirov *et al.*, 1998; Kovalenko *et al.*, 1999; Antipin *et al.*, 2002; Dobretsov, 2003; Vladimirov, 2003; Yarmolyuk and Kovalenko, 2003; Letnikov, 2003). In this context, the Kalguty rare-metal granite massif comprising an ongonite–elvan dike swarm and associated large rare-metal–molybdenum–tungsten deposit (Sotnikov and Nikitina, 1971; Dergachev and Annikova, 1988; Vladimirov *et al.*, 1997, 1998) is very interesting. Thermobarogeochemical studies demonstrated that the Kalguty ore-magmatic system shows distinct evidence of interaction between crustal and mantle melts accompanied the crystal fractionation of rare-metal granite magma in a deep-seated chamber (Annikova, 2003). This is pronounced in abrupt increase of near-liquidus crystallization temperature with transition from early plutonic to late dike stage. Homogenization temperatures of melt inclusions in quartz (T_{MI}) from rocks of the series of granites of the main phase–leucogranites of supplementary intrusions–aplites of the final phase gradually decrease from 730 to 690°C, then T_{MI} rises to 800–770°C in quartz of granite porphyry, ongonite, and elvan dikes, and drops again to 740–690°C in quartz of the late stages (Titov *et al.*, 2001). The estimated *P–T* parameters of melt crystallization cannot be accounted for by differentiation of one granite magma chamber and previous isotopic and geochemical data were insufficient to trace the whole evolution of the Kalguty ore-magmatic system.

Results of the first Rb–Sr isotopic study of the Kalguty ore-magmatic system were obtained for collection including whole-rock samples of granites of the main phase of the Kalguty complex and minerals separated from them (potassium feldspar, biotite, apatite), as well as samples of elvans and ongonites of the Eastern Kalguty complex. It was suggested that the plotted isochron (T = 204 ± 1.6 Ma; $(^{87}Sr/^{86}Sr)_0$ = 0.70688 ± 14; MSWD = 0.22; Table 4) corresponds to the time of formation of the Kalguty ore-magmatic system as an one-stage magmatic process related to activity of one lower crustal chamber and its deep differentiation (Vladimirov *et al.*, 1997). However, it is obvious now that this age value corresponds to the latest stage in evolution of the Kalguty ore-magmatic system, i.e., to the formation of the Eastern Kalguty elvan and ongonite dike complex. These rocks have the highest Rb/Sr ratios of 48–108 and, together with biotite (Rb/Sr ≥ 400), determine general slope of the line in the $^{87}Rb/^{86}Sr$–$^{87}Sr/^{86}Sr$ diagram. However, it is a pseudoiso-

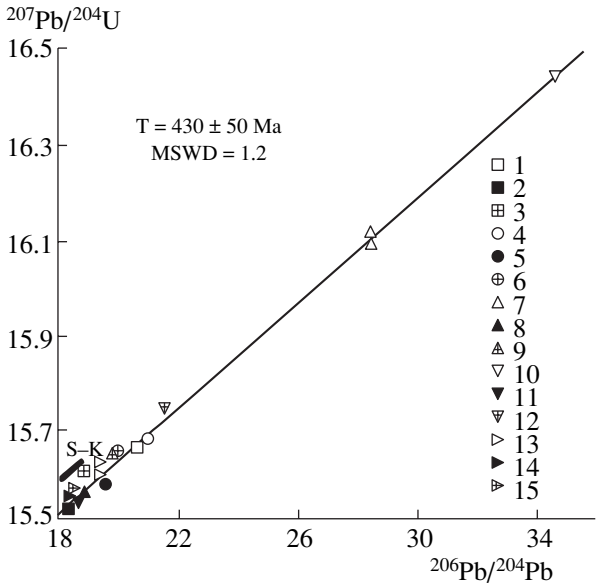

Fig. 11. $^{207}Pb/^{204}Pb$–$^{206}Pb/^{204}Pb$ diagram for untreated rock samples, leachates, and leaching residues of rocks of the Kalguty rare-metal granite massif.

(1) Sample 1-277, fraction L; (2) sample 1-277, fraction R; (3) sample 1-277, fraction WR; (4) sample 1-259, fraction L; (5) sample 1-259, fraction R; (6) sample 1-259, fraction WR; (7) sample 1-262/3, fraction L; (8) sample 1-262/3, fraction R; (9) sample 1-262/3, fraction WR; (10) sample 1-278/1, fraction L; (11) sample 1-278/1, fraction R; (12) sample 1-278/1, fraction WR; (13) sample 1-269, fraction L; (14) sample 1-269, fraction R; (15) sample 1-269, fraction WR. Samples and fractions are described in Table 3. S–K is Stacey and Kramers model line.

Table 4. Rb–Sr isotopic composition of granitoids of the Kalguty massif

Ordinal	Sample	Rock, mineral	Rb, ppm	Sr, ppm	$^{87}Rb/^{86}Sr$	$^{87}Sr/^{86}Sr$
1	SK-1/1	Granite of the main phase	355	150	6.93	0.72703 ± 11
2	SK-1/2	Feldspar	324	225	4.23	0.71978 ± 12
3	SK-1/3	Biotite	1550	12.4	407	1.81567 ± 34
4	SK-1/4	Apatite	–	226	–	0.70795 ± 10
5	5-446	Elvan	731	19.8	107	1.01763 ± 14
6	5-447	Kalgutite	1450	87.7	47.8	0.84573 ± 12

Note: Dash denotes no data.

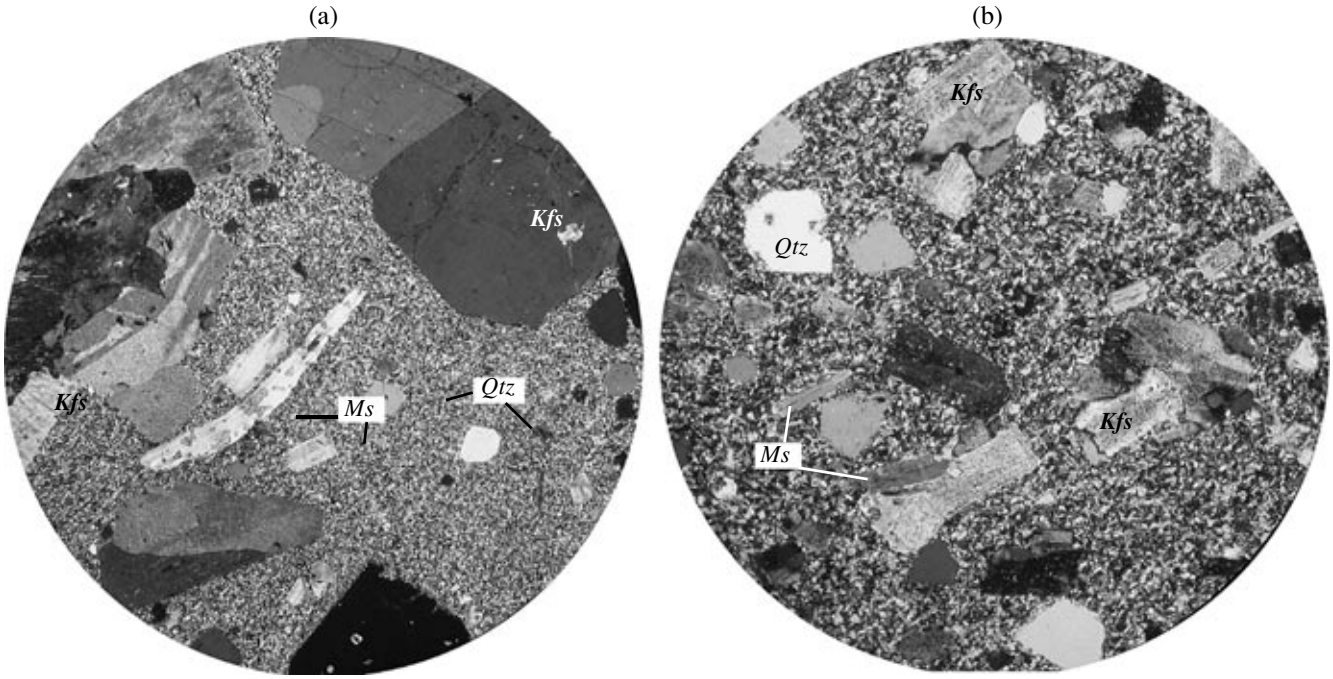

Fig. 12. Microphotographs of elvan (a) and kalgutite (b). *Ms*—muscovite, *Qtz*—quartz, *Kfs*—potassium feldspar.

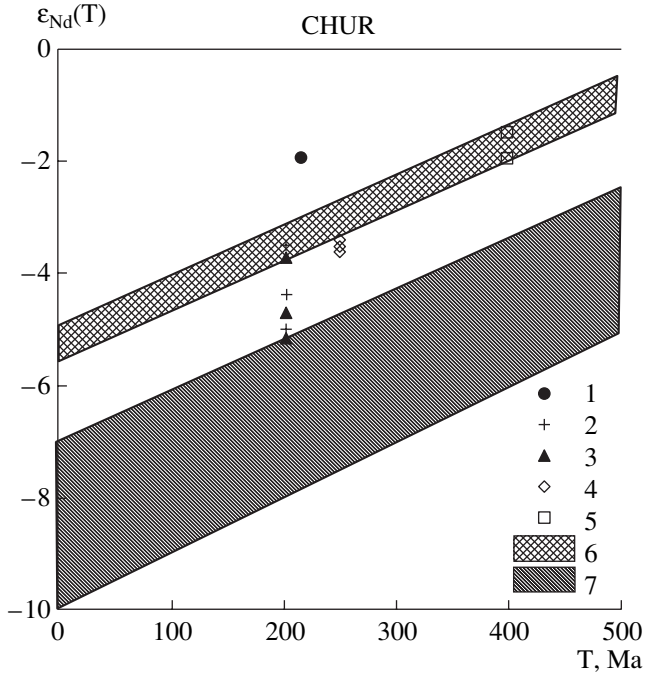

Fig. 13. $\varepsilon_{Nd}(T)$–age diagram for igneous and metamorphic rocks in the Southern Gornyi Altai Range.

(1) Granite of the main phase of the Kalguty massif; (2, 3) rocks of the Eastern Kalguty dike swarm: (2) elvans and (3) ongonites; (4) rocks of the Chuya alkali basalt complex (P_2–T_1); (5) granitoids of the Rakhmanovo complex (D_{1-2}); (6, 7) fields of evolution of isotopic composition of substrate of granitoids of the Rakhmanovo complex (6) and upper crustal metamorphic rocks of the Altai–Mongolian terrane (7).

chron, because it is based on characteristics of disturbed Rb–Sr system in biotite from granites of the main phase of the Kalguty ore-magmatic system (samples were collected within the ore field). After recalculation of Sr isotope ratio in whole-rock samples of granites of the main phase of the Kalguty complex to 216 ± 3 Ma and ongonites of the Eastern Kalguty complex to 202 ± 1 Ma, we obtained the following $(^{87}Sr/^{86}Sr)_0$ values: 0.706 ± 0.005 for granite of the main phase (sample SK-1/1), 0.711 ± 0.0035 for kalgutite (sample 5-447), and 0.710 ± 0.0035 for elvan (sample 5-446), which are close to $(^{87}Sr/^{86}Sr)_0$ value in apatite (0.708) from granites of the main phase. Estimates of primary Sr isotopic ratios (0.706–0.711) for two-stage model of evolution of the Kalguty ore-magmatic system do not show regular changes with transition from the early to late magmatic stages. We believe that this is related to insufficient experimental data and variable factors affecting the Rb–Sr system, which complicate interpretation of compositions of magma sources. Data for the Sm–Nd isotopic system are more certain.

The metamorphic rocks of the Altai–Mongolian terrane corresponding to the lowest erosion levels always have low Nd isotopic ratios and model ages of 1.5–1.7 Ga (Kruk *et al.*, 1999; Plotnikov *et al.*, 2002). These rocks present greenschist facies metasediments of the Vendian–Cambrian turbidite sequences and the Early–Middle Paleozoic Southern Chuya polymetamorphic complex with protolith model ages of 1.5–1.7 Ga and $\varepsilon_{Nd}(T) = -5$ to –8 (for the time of formation of the Kalguty ore-magmatic system). Similar model ages are typical of autochthonous granitoids emplaced during the peak of

metamorphism and granite formation in the Southern Chuya polymetamorphic complex (Plotnikov *et al.*, 2002). The Devonian calc-alkaline granitoid batoliths within the Altai–Mongolian terrane have $\varepsilon_{Nd}(T)$ from –1.5 to –2.0 and model ages of 1.3–1.35 Ga. Late Paleozoic–Early Mesozoic alkali basalts, lamprophyres, and their differentiates in this region have $\varepsilon_{Nd}(T)$ of about –3.5 and $T_{Nd}(DM)$ = 1.1–1.3 Ga.

General evolution of Nd isotopic composition in crustal substrates and igneous rocks of the Altai–Mongolian terrane is shown in Fig. 13. It shows that $^{143}Nd/^{144}Nd$ ratio in granites of the main phase of the Kalguty massif is significantly higher than that in all studied granitoids and upper crustal rocks for that time. This may indicate significant contribution of lower crustal complexes in source of granitoids. These complexes are not exposed now in the Altai–Mongolian terrane and are probably included in the Late Vendian–Early Paleozoic accretionary prism, which is found as relicts in peripheral part of the terrane (Volkova, 2003; Volkova *et al.*, 2004).

Strong decrease of primary Nd isotopic ratios and $\varepsilon_{Nd}(T)$ values in rocks of the Eastern Kalguty dike swarm (Fig. 13) can be accounted for only by participation of mantle components in magma generation. These data are probably most consistent with the suggestion of release of residual chambers of strongly evolved silicic magmas and, consequently, direct interaction of ongonite melts with a mantle chamber with "plume" isotopic characteristics.

Similarity in Nd isotopic composition of lamprophyres and high-temperature elvans (Table 2, Fig. 13) (contribution of mantle melts in these rocks is demonstrated by thermobarogeochemical methods; Titov *et al.*, 2001) is also consistent with this suggestion. Lead isotopic composition also indicates notable contribution of mantle components in the magma- and ore-forming processes in the Kalguty ore-magmatic system. We cannot exclude that isotopic composition of dike rocks was modified by assimilation of upper crustal rocks (see data for xenogenic zircon cores). However, this process might be subordinate.

Finally, let us emphasize that there is no significant correlation between Nd isotopic composition and geochemical features of rocks (e.g., their rare-metal contents). This fact verifies the idea that the rare-metal composition of rocks of the Eastern Kalguty dike swarm was generally determined by direction and degree of differentiation of parental magmas, rather than contribution of mantle components.

CONCLUSIONS

Two intrusive complexes can be distinguished in structure of the Kalguty ore-magmatic system, i.e., Kalguty granite–leucogranite complex and Eastern Kalguty complex of dikes and small intrusions. The earlier stage is represented by granites (90%), leucogranites (10%), and veins of aplites and pegmatites, while the later stage, by granite porphyry with elevated rare-metal contents, apatite-bearing elvans, and ongonites. U–Pb dating of individual zircon grains from granites of the main intrusive phase demonstrated that the crystallization age of small grains of magmatic habits and outer rims of large grains is almost concordant and is 216 ± 3 Ma. Some zircon grains are xenogenic and have age of about 400–440 Ma. These grains were probably derived from xenoliths of the Early Devonian volcanic rocks assimilated by granite magma. Ar–Ar isotope study shows that the K–Ar system of biotites from granites of the main phase within the Kalguty ore field was disturbed (radiogenic Ar was partially lost) and gave an age of 202 ± 1 Ma. The Ar–Ar dating of muscovites from intraore and postore ongonite and elvan dikes of the Eastern Kalguty complex devoid of signatures of postmagmatic recrystallization and superimposed greisenization gave similar ages of 205–201 Ma. This date is interpreted as the emplacement age of the Eastern Kalguty dikes and associated complex W–Mo–Bi–Be ore mineralization. Similarity of underestimated Ar–Ar ages of biotites from altered granites and muscovites from unaltered ongonites and elvans can be explained by heating of ore-hosting rocks above 250°C (closure temperature of K–Ar system in biotite).

Sm–Nd and Pb–Pb isotopic study of granites, ongonites, and elvans of the Kalguty ore-magmatic system and host rocks show that these systems, like the U–Pb systems of zircon, were closed. For example, recalculation of Nd isotopic ratios for corresponding ages of crystallization of magmatic systems (216 and 205 Ma) shows that $\varepsilon_{Nd}(T)$ values decrease from –1.9 to –3.5 … –5.08 with transition from granite–leucogranite to subvolcanic granite porphyry, ongonite, and elvan dikes with corresponding increase of model ages of protoliths from 1.0 to 1.25 Ga. Because the Kalguty ore-magmatic system was formed by activity of single crustal chamber, shift of Nd isotopic compositions could be explained only by influence of mantle source. Lead isotopic ratios for leaching residues of whole-rock samples of all rock varieties ($^{206}Pb/^{204}Pb$ = 18.305–18.831; $^{207}Pb/^{206}Pb$ = 15.527–15.571) are plotted well below the line of average crustal lead evolution according to the Stacey–Kramers model. This is consistent with anomalously high temperatures of the Eastern Kalguty dikes determined by melt inclusions in quartz, which could be accounted for by impact of mantle sources on the evolved lower crustal granite chamber.

ACKNOWLEDGMENTS

The authors thank V.S. Antipin (Vinogradov Institute of Geochemistry, Siberian Division, Russian Academy of Sciences), A.S. Borisenko and A.A. Obolenskii (Institute of Geology, Siberian Division, RAS), S.P. Shokal'skii (Karpinskii All-Russia Research Institute of Geology), A.B. Kotov and G.V. Ovchinnikova (Institute of Precambrian Geology and Geochronology,

RAS), and V.V. Yarmolyuk (Institute of Ore Deposits, Petrography, Mineralogy and Geochemistry, RAS) for fruitful remarks during preparation of the manuscript.

The study was supported by Program of Basic Research of Siberian Division of Russian Academy of Sciences "Geodynamic evolution of the Central Asian mobile belt" (project no. 6.7.2), Presidium of Siberian Division of Russian Academy of Sciences (project no. 106), Russian Foundation for Basic Research (project nos. 03-05-65099, 04-05-64443), and Ministry of Education and Science of Russia (project UR.09.01.212).

REFERENCES

1. N. N. Amshinskii, *Vertical Petrogeochemical Zoning of Granitoid Plutons* (Zap. Sib. Knizh. Izd., Novosibirsk, 1973) [in Russian].
2. I. Yu. Annikova, A. G. Vladimirov, S. A. Vystavnoi, *et al.*, "Geological–Geophysical Formation Model of the Kalguty Ore–Magmatic System, Southern Altai," Izv. Tomsk. Politekh. Univ. **307** (4), 45–56 (2004).
3. I. Yu. Annikova, Extended Abstract of Candidate's Dissertation in Geology and Mineralogy (Inst. Geol., Sib. Otd. Ross. Akad. Nauk, Novosibirsk, 2003).
4. I. Yu. Annikova, V. B. Dergachev, and V. N. Terekhov, "The Interrelation of Rare Metal Granites, Ongonites, and Ore Mineralization in the Kalguty Massif, Gornyi Altai," in *Abstracts of Papers of Scientific–Applied Conference "Geological Structure and Mineral Deposits of Western Altai–Sayan Folded Belt"* (Novokuznetsk, 1999), pp. 220–222 [in Russian].
5. V. S. Antipin, C. Halls, M. A. Mitichkin, *et al.*, "Elvans of Cornwall (England) and Southern Siberia as Subvolcanic Counterparts of Subalkalic Rare Metal Granites," Geol. Geofiz. **43** (9), 847–857 (2002).
6. J. A. Aque and G. H. Brimhall, "Granites of the Batholiths of California: Products of Local Assimilation and Regional-scale Crustal Contamination," Geology **15**, 63–66 (1987).
7. N. A. Berzin, R. G. Coleman, N. L. Dobretsov, *et al.*, "Geodynamic Map of the Western Zone of Paleoasian Ocean," Geol. Geofiz. **35** (7–8), 8–28 (1994).
8. L. P. Black, S. L. Kamo, *et al.*, "TEMORA 1: A New Zircon Standard for U–Pb Geochronology," Chem. Geol. **200**, 155–170 (2003).
9. A. S. Borisenko, A. A. Borovikov, G. G. Pavlova, and L. V. Gushchina, "Sn–Ag Ore-forming Systems," in *Proceedings of the Seventh Biennial SGA Meeting "Mineral Exploration and Sustainable Development," Athens, August 24–28, 2003* (Millpress, Rotterdam, 2003), Vol. 1, pp. 251–254.
10. S. V. Budnikov, G. H. Brimhall, C. D. Lewis, *et al.*, "Typification of Mongolian Granitoids on Mica Composition and Its Use in Distinguishing Magmatic Associations," Dokl. Akad. Nauk **333** (2), 207–209 (1993).
11. M. M. Buslov, T. Watanabe, L. V. Smirnova, *et al.*, "Role of Strike-slip Faults in Late Paleozoic–Early Mesozoic Tectonics and Geodynamics of the Altai–Sayan and East Kazakhstan Folded Belts," Geol. Geofiz. **44** (1–2), 49–75 (2003).
12. G. E. Dashkevich, N. K. Mortsev, and A. A. Borovikov, "Explosive Breccias of the Kalguty Deposit, Gornyi Altai," in *Petrology, Geochemistry, and Ore-bearing Potential of Southern Siberian Intrusive Complexes* (Ob"ed. Inst. Geol. Geofiz. Mineral., Sib. Otd. Russ. Akad. Nauk, Novosibirsk, 1991), pp. 44–49 [in Russian].
13. V. B. Dergachev and I. Yu. Annikova, "Petrogeochemical Composition and Zoning of Rare Metal Dike Belt," in *Zoning and Formation Conditions of Siberian Ore Deposits* (Sib. Nauchno-Issled. Inst. Geol. Geophys. Mineral. Syr'ya, Novosibirsk, 1988), pp. 21–31 [in Russian].
14. V. B. Dergachev, "A New Variety of Ongonites," Dokl. Akad. Nauk SSSR **302** (1), 188–191 (1988).
15. N. L. Dobretsov, "Mantle Plumes and Their Role in Formation of Anorogenic Granitoids," in *The Current Problems of Formation Analysis and the Petrology and Ore-bearing Potential of Magmatic Rocks* (Sib. Otd. Ross. Akad. Nauk, Novosibirsk, 2003) [in Russian].
16. R. J. Fleach, J. F. Sutter, and D. H. Elliot, "Interpretation of Discordant $^{40}Ar/^{39}Ar$ Age Spectra of Mesozoic Tholeiites from Antarctica," Geochim. Cosmochim. Acta **41**, 15–32 (1977).
17. S. J. Goldstein and S. B. Jacobsen, "Nd and Sr Isotopic Systematics of Rivers Water Suspended Material: Implications for Crustal Evolution," Earth Planet. Sci. Lett. **87**, 249–265 (1988).
18. V. A. Il'in, V. A. Khalilov, M. S. Kozlov, *et al.*, "U–Pb and Rb–Sr Dating of the Alakha Stock, Gornyi Altai," Geol. Geofiz., No. 1, 79–81 (1994).
19. S. B. Jacobsen and G. J. Wasserburg, "Sm–Nd Evolution of Chondrites and Achondrites," Earth Planet. Sci. Lett. **67**, 137–150 (1984).
20. Yu. A. Kostitsyn, S. A. Vystavnoi, and A. G. Vladimirov, "Age and Genesis of the Spodumene-bearing Granites of the SW Altai, Russia: An Isotopic and Geochemical Study," Acta Univ. Carolinae, Geologica **42** (1), 60–63 (1998).
21. V. I. Kovalenko, *Petrology and Geochemistry of Rare Metal Granitoids* (Nauka, Novosibirsk, 1977) [in Russian].
22. V. I. Kovalenko, Yu. A. Kostitsyn, V. V. Yarmolyuk, *et al.*, "Magma Sources and the Isotopic (Sr and Nd) Evolution of Li-F Rare-Metal Granites," Petrologiya **7** (4), 401–429 (1999) [Petrology **7** (4), 383–409 (1999)].
23. M. S. Kozlov, V. A. Khalilov, N. V. Stasenko, and V. I. Timkin, "Jurassic Leucogranite–Granite Association in the Altai Region," Geol. Geofiz., No. 8, 43–52 (1991).
24. N. N. Kruk, S. N. Rudnev, A. G. Vladimirov, and D. Z. Zhuravlev, "Sm–Nd Isotope Systematics of Granitoids from the Western Altai-Sayan Fold Zone," Dokl. Akad. Nauk **366** (3), 395–397 (1999) [Dokl. Earth Sci. **366** (4), 569–571 (1999)].
25. F. A. Letnikov, "The Fluid Regime of Endogenic Processes in the Continental Lithosphere and the Problem of Origin and Ore-bearing Potential of Magmatic Rock Associations," in *The Current Problems of Formation Analysis and the Petrology and Ore-bearing Potential of Magmatic Rocks* (Sib. Otd. Ross. Akad. Nauk, Novosibirsk, 2003) [in Russian].
26. T. C. Liew and A. W. Hofmann, "Precambrian Crustal Components, Plutonic Associations, and Plate Environment of the Hercynian Fold Belt of Central Europe: Indi-

cations from a Nd and Sr Isotopic Study," Contrib. Mineral. Petrol. **98**, 129–138 (1988).

27. K. R. Ludwig, "SQUID 1.00: A User's Manual," Berkeley Geochronol. Center Spec. Publ., No. 2 (2000).
28. K. R. Ludwig, "User's Manual for Isoplot/Ex. Version 2.10. A Geochronological Toolkit for Microsoft Excel," Berkeley Geochronol. Center Spec. Publ., No. 1a, (1999).
29. B. N. Luzgin, "A Spatial Model of Ore Mineralization for the Kalguty Ore Region, Gornyi Altai," Sov. Geol., No. 8, 94–97 (1988).
30. G. Manhes, C. J. Allegre, and A. Provost, "U–Th–Pb Systematics of the Sucrite "Juvinas": Precise Age Determination and Evidence for Exotic Lead," Geochim. Cosmochim. Acta **48** (12), 2247–2264 (1984).
31. O. A. Morozov, "K–Ar Dating of the Kalguty Granite Pluton," Izv. Akad. Nauk SSSR, Ser. Geol., No. 10, 145–149 (1986).
32. A. V. Plotnikov, N. N. Kruk, A. G. Vladimirov, *et al.*, "Sm–Nd Isotope Systematics of Metamorphic Rocks in the Western Altai–Sayan Fold Belt," Dokl. Akad. Nauk **388** (2), 228–232 (2002) [Dokl. Earth Sci. **388** (1), 63–67 (2003)].
33. P. Richard, N. Shimizu, and C. J. Allegre, "$^{143}Nd/^{144}Nd$ Natural Tracer: An Application to Oceanic Basalts," Earth Planet. Sci. Lett. **31**, 269–278 (1976).
34. S. P. Shokal'skii, G. A. Babin, A. G. Vladimirov, *et al.*, *The Correlation of Magmatic and Metamorphic Complexes in West Altai–Sayan Folded Belt* (Sib. Otd. Ross. Akad. Nauk, Novosibirsk, 2000) [in Russian].
35. V. I. Sotnikov and E. I. Nikitina, *Greisen-related Molybdenum–Rare-metal–Tungsten Deposits in Gornyi Altai* (Nauka, Novosibirsk, 1971) [in Russian].
36. R. N. Steiger and E. Jager, "Subcomission on Geochronology: Convention and Use of Decay Constants in Geo- and Cosmochronology," Earth Planet. Sci. Lett. **36**, 359–362 (1976).
37. S. R. Taylor and S. M. McLennan, *The Continental Crust: Its Composition and Evolution* (Blackwell, Oxford, 1985; Mir, Moscow, 1988).
38. A. V. Titov, A. G. Vladimirov, S. A. Vystavnoi, and L. N. Pospelova, "Extraordinary High-Temperature Felsite Porphyries in the Postgranite Dike Swarm of the Kalguty Rare-metal Granite Massif, Gornyi Altai Mountains," Geokhimiya, No. 6, 677–682 (2001) [Geochem. Int. **39** (6), 615–620 (2001)].
39. A. V. Travin, Extended Abstract of Candidate's Dissertation in Geology and Mineralogy (Ob"ed. Inst. Geol. Geophys. Mineral., Sib. Otd. Ross. Akad. Nauk, Novosibirsk, 1994).
40. A. G. Vladimirov, "Collision Tectonics and Magmatic Rock Associations," in *The Current Problems of Formation Analysis and the Petrology and Ore-bearing Potential of Magmatic Rocks* (Sib. Otd. Ross. Akad. Nauk, Novosibirsk, 2003) [in Russian].
41. A. G. Vladimirov, A. P. Ponomareva, S. P. Shokal'skii, *et al.*, "Late Paleozoic to Early Mesozoic Granitoid Magmatism in the Altai Region," Geol. Geofiz., No. 4, 715–729 (1997).
42. A. G. Vladimirov, S. A. Vystavnoi, A. V. Titov, *et al.*, "The Petrology of Early Mesozoic Rare-metal Granitoids in South Gornyi Altai: Insight into the Problem of Magmas Enriched in Rare Alkalis and Phosphorus," Geol. Geofiz. **39** (7), 901–916 (1998).
43. N. I. Volkova, "Geochemistry and Protolith Nature of Metabasites from the Terekty Blueschist–Greenschist Complex (Gorny Altai)," Dokl. Akad. Nauk **393** (2), 224–226 (2003) [Dokl. Earth Sci. **393** (8), 1170–1173 (2003)].
44. N. I. Volkova, S. I. Stupakov, V. A. Simonov, and Yu. V. Tikunov, "Petrology of Metabasites from Terekta Complex as Constituent of Ancient Accretionary Prism of Gorny Altai," J. Asian Earth Sci. **23** (5), 705–713 (2004).
45. I. S. Williams, "U–Th–Pb Geochronology by Ion Microprobe," in *Applications of Microanalytical Techniques to Understanding Mineralizing Processes*, Ed. by M. A. McKibben, W. C. Shanks III, and W. I. Ridley, Rev. Econ. Geol. **7**, 1–35 (1998).
46. V. V. Yarmolyuk and V. I. Kovalenko, "Batholiths and Dynamics of Batholith Formation in the Central Asian Folded Belt," in *The Current Problems of Formation Analysis and the Petrology and Ore-bearing Potential of Magmatic Rocks* (Sib. Otd. Ross. Akad. Nauk, Novosibirsk, 2003) [in Russian].